Eur. Phys. J. D (2020) 74: 173
https://doi.org/10.1140/epjd/e2020-10226-1

THE EUROPEAN PHYSICAL JOURNAL D

Regular Article

Small recoil momenta double ionization of He and two-electron ions by high energy photons

Miron Ya. Amusia[1,2], Evgenii G. Drukarev[3], and Evgeny Z. Liverts[1,a]

[1] Racah Institute of Physics, The Hebrew University, Jerusalem 91904, Israel
[2] A. F. Ioffe Physical-Technical Institute, St. Petersburg 194021, Russia
[3] National Research Center "Kurchatov Institute" B. P. Konstantinov Petersburg Nuclear Physics Institute, Gatchina, St. Petersburg 188300, Russia

Received 18 April 2020 / Received in final form 13 June 2020
Published online 25 August 2020

Abstract. We calculate various differential and double differential characteristics of ionization by a single photon for H^-, He and for the two-electron ions with $Z = 3, 4, 5$ in the region of the so-called quasi-free mechanism (QFM) domination. We employ highly accurate wave functions at the electron-electron coalescence line where coordinates of both ionized electrons coincide. We trace the Z dependence of the double differential distributions. For all considered targets we discuss the dependence of the photoelectron energy distribution on the photon energy. Our calculation demonstrated the rapid decrease of QFM contribution with increase of the difference in energy of two outgoing electrons, and with decrease of the angle between two outgoing momenta. As a general feature, we observe the decrease of QFM contribution with nuclear charge growth.

1 Introduction

By "high energy photoionization" we mean absorption of photons with energies ω much exceeding the single electron binding energies I, i.e. $\omega \gg I$. If only one photoelectron is emitted, the momentum transferred to the nucleus that is called the recoil momentum q, is estimated as $q \approx p$ with p being the momentum in high energy photoionization of photoelectrons. Thus, the recoil momentum strongly exceeds the characteristic binding momentum of the ionized object $\mu = (2mI)^{1/2}$ with m being the electron mass (we employ the relativistic system of units with $\hbar = c = 1$), i.e. $q \gg \mu$. This is because photoionization with only one electron knocked out cannot take place on a free electron.

Similar situation takes place for the double photoionization, in emission of two electrons by a single photon, if the photon energy ω is not too large. The sharing of energy is strongly unequal and $q \approx p_1 \approx (2m\omega)^{1/2}$ with p_1 standing for momentum of the faster photoelectron, while the second electron is emitted with momentum $p_2 \sim \mu$. However, with the increase of ω the role of so-called quasi-free mechanism (QFM) suggested in [1] becomes more and more important. In the frame of QFM momenta of photoelectrons $\mathbf{p}_{1,2}$ and that of the photon $\mathbf{k}$ compose such configuration that the recoil momentum

$$\mathbf{q} = \mathbf{k} - \mathbf{p}_1 - \mathbf{p}_2, \tag{1}$$

becomes as small as the binding momentum μ, i.e.

$$q \sim \mu. \tag{2}$$

Since each act of transfer of large momentum $q \gg \mu$ to the nucleus leads to the small factor $1/q^2$ in the amplitude, the QFM provides surplus in differential characteristics and in the total cross section of double ionization.

Most of the publications on QFM touched the theory of the mechanism for the case of two-electron (helium-like) atomic systems. In the first calculation of the QFM contribution to the total double photoionization cross section [2] it was shown to become the main mechanism of the process at the energies of hundreds keV for He. The nuclear charge dependence of QFM contribution to the cross section was traced in [3]. It was emphasized in [4] that the description of the QFM requires employing the two-electron bound state wave function $\psi(\mathbf{r}_1, \mathbf{r}_2)$ with the proper analytical behavior on the electron-electron coalescence line $\mathbf{r}_1 = \mathbf{r}_2$. The relation between the precise two-electron wave function and its coordinate derivative at the line of zero interelectron distance is known as the second Kato's cusp condition [5]. The fulfillment of this condition in calculations usually employed to approximate wave functions is necessary for proper description of QFM since it accounts for the singularity of the Coulomb interelectron interaction. For more details and references see Chapter 9 of the book [6].

It follows from the works mentioned above that for helium the QFM provides a noticeable contribution to the

[a] e-mail: liverts@phys.huji.ac.il

spectrum of photoelectrons starting from the photon energies of about 2 keV. The QFM corrections to the total cross section become noticeable at the photon energies of dozens keV. For heavier two-electron ions the corresponding photon energies become larger. As it stands now, experimental data for such energies are not available.

Although the QFM was discussed in literature during many years, to detect it experimentally remained a challenge until this was done by the group of Dörner [7]. Note that this discovery was made 38 years after its prediction [1] and became possible only after invention of a new experimental technique which enables investigation into the double electron photoionization as a function of recoil momentum q. However, the obtained clear manifestation of the QFM has been detected at a much smaller value of the photon energy $\omega = 800$ eV than expected. It was found in [7] that the distribution in momenta q transferred to the final state doubly charged ions in double photoionization of helium has a surplus at small q of about 1−2 atomic units. It was impossible, however, to compare experiment with theory since reference [7] did not contain absolute measured values.

Note that the QFM can not take place in dipole approximation. It requires inclusion of the quadrupole interaction. Theoretical investigation into the contribution of quadrupole effects was continued, e.g. by the papers [8–10]. The development of experimental technique [11], [12] enabled to separate the dipole and quadrupole contributions in the experiments on the double photoionization [13]. This demonstrates that investigation into the double electron ionization by a single photon as a function of recoil momentum becomes an important tool in studies of short-range interelectron correlations in atoms and in perspective, in molecules as well as even more complex compounds.

An important move mainly in experimental investigation and not only of helium atom but of hydrogen molecule also has been made by the quite recent publication [14]. In [14] the double differential distributions $d^2\sigma/d\tau d\beta$ with $\tau = \mathbf{p}_1\mathbf{p}_2/p_1p_2$ and

$$\beta = \frac{|\epsilon_1 - \epsilon_2|}{E}, \tag{3}$$

($\varepsilon_{1,2}$ are the energies of the photoelectrons, $E = \varepsilon_1 + \varepsilon_2 = \omega - I^{++}$, where I^{++} is the two-electron ionization potential) have been measured for He atom and H_2 molecule. Quite a powerful QFM peak at $\tau = -1$, $\beta = 0$ has been observed in both objects. Also the peak in the energy distribution

$$\frac{d\sigma}{d\beta} = \int_{(p_1-p_2)^2}^{(p_1+p_2)^2} \left(\frac{d^2\sigma}{dq^2 d\beta}\right) d(q^2) \tag{4}$$

has been seen for the same targets attributed to QFM.

These results prompt theoretical investigation into QFM for other, not yet investigated two-electron systems that can become the objects of photoionization studies soon. Note that the results of [7] stimulated us to calculate the differential distributions of the process for He atom at $q \sim \mu$ and photon energies $\omega \approx 1$ keV [15]. In [15] we employed approximate bound state wave functions at the electron-electron coalescence line obtained in the work [16]. This enabled us to carry out analytical calculations.

Since then the ability to calculate improved considerably. So, in the present paper, we employ much more sophisticated bound state wave functions [17,18] having in mind the impressive increase in experimental accuracy achieved in [14]. We also extend our calculations to include all the lightest two-electron positive ions ($Z \leq 5$) and the negative hydrogen ion H^-. For He atom we trace the dependence of the double differential distributions on the photon energy ω. Including several two-electron ions, we trace the Z dependence of the double differential contributions for photon energies around 1 keV.

While we consider the photon energies corresponding to nonrelativistic photoelectrons, i.e. $\omega \ll m$, the QFM is possible only in the vicinity of the center of the energy distribution, where the relative difference of the electron energies β is small, $\beta \ll 1$. The actual value of $\varepsilon_1 - \varepsilon_2$ where the QFM is possible depends on the ratio k/μ of the photon momentum $k = \omega$ and of the characteristic momentum of the bound state μ [1]. We consider the case $\omega \ll \mu$. For helium this means $\omega \ll 6$ keV. In this case $p_1 - p_2 \leq q$ and the QFM is at work if

$$\beta \leq \sqrt{\frac{q^2}{mE}}. \tag{5}$$

Condition (2) requires also that the photoelectrons move in approximately opposite directions since $\tau = \mathbf{p}_1\mathbf{p}_2/p_1p_2 = (q^2 - p_1^2 - p_2^2)/(2p_1p_2) \approx -1$.

An important feature of the QFM is that its amplitude F can be expressed in terms of the amplitude F_0 that represents moving to continuum due to the photon absorption by two free electrons at rest (see below and [6]). This explains the name "quasifree"- the two-electron system cam move almost without noticing the nucleus. However to do this the motion of the electrons should be strongly correlated.

One can see that the QFM is impossible in the dipole approximation where we must put $\mathbf{k} = 0$. In this case the photoelectrons move exactly bach-to-back with $\mathbf{p}_1 + \mathbf{p}_2 = 0$. The incoming photon carries spin $S = 1$ while the two-electron system in spin singlet state can not carry angular momentum $J = 1$. Thus, we must include the quadrupole terms of interaction between the photon and electrons.

Presenting $\varepsilon_2 = (\mathbf{p}_1 - \mathbf{q})^2/2m$ we find for the differential cross section corresponding to the QFM

$$d\sigma = 2\pi\delta\Big(E - 2\varepsilon_1 - \frac{p_1 q_z}{m} - \frac{q^2}{2m}\Big)|F|^2 \frac{d^3p_1}{(2\pi)^3}\frac{dq^2 dq_z}{4\pi}. \tag{6}$$

Here F is the amplitude describing the QFM mechanism; the averaging over photon polarizations should be carried out. Also, z is the direction of momentum $\mathbf{p}_1 - \mathbf{k}$, and we put $\mathbf{p}_1 - \mathbf{k} \simeq \mathbf{p}_1$ in the argument of the delta-function. Using the delta-function for integration over q_z we obtain for the double differential distribution

$$\frac{d^2\sigma}{dq^2 d\beta} = \frac{m^2 E}{2}\int \frac{|F|^2\, dt}{(2\pi)^3}; \quad t = \mathbf{p}_1\mathbf{k}/p_1 k. \tag{7}$$

Another double differential distribution of interest is

$$\frac{d^2\sigma}{d\tau d\beta} = 2p_1p_2\frac{d^2\sigma}{dq^2d\beta} = m^2E^3\int\frac{|F|^2}{(2\pi)^3}dt. \quad (8)$$

Employing these expressions, one can obtain other differential distributions, e.g.

$$\frac{d\sigma}{dq^2} = \frac{1}{2}\int_0^{q/p}d\beta\frac{d^2\sigma}{dq^2d\beta}; \quad p=(mE)^{1/2}. \quad (9)$$

2 The QFM amplitude

We introduce

$$\mathbf{R}=(\mathbf{r}_1+\mathbf{r}_2)/2; \quad \boldsymbol{\rho}=\mathbf{r}_1-\mathbf{r}_2, \quad (10)$$

with $\mathbf{r}_{1,2}$ denoting the positions of the two electrons in the rest frame of the nucleus. We present the ground state wave function in terms of these variables

$$\Psi(\mathbf{r}_1,\mathbf{r}_2) = \hat{\Psi}(\mathbf{R},\boldsymbol{\rho}). \quad (11)$$

It is instructive to start with the QFM amplitude $F^{(0)}$ in which the photoelectrons are described by the plane waves. Thus, the wave function of the photoelectrons is

$$\Psi_{ph}(\mathbf{r}_1,\mathbf{r}_2) = \frac{1}{\sqrt{2}}\Big(\psi_{p_1}(\mathbf{r_1})\psi_{p_2}(\mathbf{r_2})+\psi_{p_1}(\mathbf{r_2})\psi_{p_2}(\mathbf{r_1})\Big), \quad (12)$$

with $\psi_{p_j}(\mathbf{r})=e^{-i\mathbf{p}_j\mathbf{r}}$. Analysis that employs such a wave function contains all essential physics.

Introducing $\boldsymbol{\kappa}=(\mathbf{p}_1-\mathbf{p}_2)/2\approx\mathbf{p}_1$ we write

$$F^{(0)}=\sqrt{2}N(\omega)\int d^3Rd^3\rho e^{-i\mathbf{qR}+i(\boldsymbol{\kappa}-\mathbf{k}/2)\cdot\boldsymbol{\rho}} \Big(\frac{i\mathbf{e}\cdot\nabla_\rho}{m}-\frac{i\mathbf{e}\cdot\nabla_R}{2m}\Big)\hat{\Psi}(\mathbf{R},\boldsymbol{\rho})+(\mathbf{p}_1\leftrightarrow\mathbf{p}_2), \quad (13)$$

with $N(\omega)=\sqrt{4\pi\alpha/2\omega}$ the normalization factor of the photon wave function. Integrating by parts we find that since $\kappa=|\boldsymbol{\kappa}|\gg q$, the first term in the parenthesis on the right hand side dominates, providing

$$F^{(0)}=\sqrt{2}N(\omega)\frac{\mathbf{e}\boldsymbol{\kappa}}{m}\int d^3Rd^3\rho e^{i\mathbf{qR}+i(\boldsymbol{\kappa}-\mathbf{k}/2)\cdot\boldsymbol{\rho}} \hat{\Psi}(\mathbf{R},\boldsymbol{\rho})+(\mathbf{p}_1\leftrightarrow\mathbf{p}_2). \quad (14)$$

The integral is determined by $R\sim 1/q\sim 1/\mu$ i.e. the characteristic R are of the order of the size of the bound state. The important values of ρ are much smaller being of the order $1/\kappa\ll 1/\mu$. To pick the quadrupole terms we present the wave function as

$$\hat{\Psi}(\mathbf{R},\boldsymbol{\rho}) = \hat{\Psi}(R,0,0)+\zeta\hat{\Psi}'(R,\zeta,0)|_{\zeta=0}+\rho\hat{\Psi}'(R,0,\rho)|_{\rho=0}+0(\rho^2), \quad (15)$$

with $\zeta=\mathbf{R}\cdot\boldsymbol{\rho}$. Substituting this expansion into the integral over ρ in equation (13)

$$J(\mathbf{a},R)=\int d^3\rho e^{i\mathbf{a}\boldsymbol{\rho}}\hat{\Psi}(\mathbf{R},\boldsymbol{\rho}), \quad (16)$$

with

$$\mathbf{a}=\frac{\mathbf{p}_1-\mathbf{p}_2-\mathbf{k}}{2} \quad (17)$$

we see that only the third term on the right hand side of equation (15) contributes, providing

$$J(\mathbf{a},R)=-\frac{8\pi\hat{\Psi}'(R,0,\rho)|_{\rho=0}}{a^4}=-\frac{4\pi m\alpha}{a^4}\hat{\Psi}(\mathbf{R},0). \quad (18)$$

The second equality is due to the second Kato cusp condition [5]

$$\frac{\partial\hat{\Psi}(\mathbf{R},\boldsymbol{\rho})}{\partial\rho}|_{\rho=0}=m\alpha\hat{\Psi}(\mathbf{R},\boldsymbol{\rho}=0)/2.$$

Thus, the amplitude

$$F^{(0)} = \sqrt{2}N(\omega)\frac{\mathbf{e}\boldsymbol{\kappa}}{m}\int d^3R\, e^{i\mathbf{qR}}J(\mathbf{a},R)+\Big(\mathbf{p}_1\leftrightarrow\mathbf{p}_2\Big) \quad (19)$$

can be written as

$$F^{(0)}=F_0S(q). \quad (20)$$

Here

$$S(q) = \int d^3re^{i\mathbf{qr}}\Psi(\mathbf{r},\mathbf{r}) = \int\frac{d^3f}{(2\pi)^3}\tilde{\Psi}(\mathbf{q}-\mathbf{f},\mathbf{f}) \quad (21)$$

describes transfer of momentum $\mathbf{q}$ from the nucleus to the bound electrons. In the lowest order of expansion in powers of I^{++}/ω we put $E=\omega$, and as a result have

$$F_0 = -4\pi\sqrt{2}\alpha N(\omega)\frac{\mathbf{e}\boldsymbol{\kappa}}{a^4}+\Big(\mathbf{p}_1\leftrightarrow\mathbf{p}_2\Big), \quad (22)$$

the amplitude of the process in which one photon moves the system consisting of two free electrons in spin-singlet state to continuum.

In the lowest (dipole) approximation we must put $\mathbf{k}=0$ in the factor $1/a^4$ with a defined by equation (17). This leads to $F_0=0$ and $F^{(0)}=0$ in agreement with the analysis presented above. The leading nonvanishing contribution is provided by next to leading term of expansion of the factor

$$\frac{1}{a^4}=\frac{1}{m^2E^2}\left(1+\frac{2\mathbf{p_1k}}{mE}\right). \quad (23)$$

Here we neglected the terms of the order β^2. Inclusion of such terms would require higher order terms of expansion of the right hand side of equation (15) in powers of ρ. Thus the amplitude of the process on free electrons is

$$F_0 = -16\pi\sqrt{2}\alpha N(\omega)\frac{(\mathbf{ep}_1)(\mathbf{p_1k})}{m^3E^3}, \quad (24)$$

where we must put $E=\omega$, while the amplitude for the process on the bound electrons is given by equation (20).

Now we describe the photoelectrons by nonrelativistic Coulomb functions. Note that we do not employ expansion

in powers of I^{++}/ω. The two-electron wave function is presented by equation (12) with

$$\psi_{p_j}(\mathbf{r}) = e^{-i\mathbf{p}_j\mathbf{r}} X_{p_j}(\mathbf{r}); \quad X_{p_j}(\mathbf{r}) = N(\xi_j)\,{}_1F_1(i\xi_j, 1, ip_jr - i\mathbf{p}_j\mathbf{r}), \tag{25}$$

where ${}_1F_1(b,1,z)$ is the confluent hypergeometric function of the first kind, $\xi_j = m\alpha Z/p_j$, $N(\xi_j) = [2\pi\xi_j/(1-e^{-2\pi\xi_j})]^{1/2} = \psi_{p_j}(\mathbf{r}=0)$. Evaluation similar to that carried out for the case when the photoelectrons are described by plane waves [15], [6], provides in the limit $E = \omega$

$$F = F_0 S_1(q,\beta)\,. \tag{26}$$

Here F_0 is given by equation (24) while

$$S_1(q,\beta) = \int d^3R e^{i\mathbf{qR}} X_{p_1}(\mathbf{R}) X_{p_2}(\mathbf{R}) \tilde{\Psi}(R,0), \tag{27}$$

see equations (20) and (21). The corrected analytical representation for the integral $S_1(q)$ is presented in the Appendix.

3 Differential distributions and the QFM cross section

Combining equations (7), (26) and (27) we find the QFM double differential distribution. It can be presented as

$$\frac{d^2\sigma}{dq^2 d\beta} = \frac{1}{\kappa}\frac{d^2\sigma_1}{dq^2 d\beta}; \quad \frac{d^2\sigma_1}{dq^2 d\beta} = \frac{2^6}{15}\alpha^3 \frac{|S_1(q)|^2}{m^2\omega^2}, \tag{28}$$

with the kinematical factor

$$\kappa = \frac{E^3}{\omega^3} = \left(\frac{\omega - I^{++}}{\omega}\right)^3.$$

Such presentation is convenient for description of the process with various targets at fixed values of ω. All effects of interactions are contained in the factor $S_1(q,\beta)$. Recall that $E = \omega - I^{++}$ is the energy carried by two photoelectrons. Here I^{++} is the total binding energy of the system containing two bound electrons.

In Figures 1–4 we present the result for helium at $\omega = 800\,\text{eV}$, changing ω for the other targets, i.e. for the negative ion H^- and for the two-electron ions with $Z = 3,4,5$, proportionally to the total binding energies I^{++}. Thus, the factor κ is the same for all these objects. The binding energies of the two-electron atomic systems are well-known and approximately equal to 14.4 eV, 78.9 eV, 198 eV, 453 eV and 599 eV for $Z = 1,2,3,4$ and 5, respectively. In atomic units they are 0.528, 2.903, 7.28, 13.66, and 22.03 (see, e.g., [16–18]).

In Figure 1 we trace the Z dependence of the distribution $d^2\sigma/dq^2 d\beta$ at the point of equal sharing $\beta = 0$. We present the results for He as well as for H^- and for the two-electron ions of the nuclei with $Z = 3,4,5$. These distributions were studied in [7] for He only. In Figure 1b we show the distribution for helium for the most studied case $\omega = 800\,\text{eV}$ [9]. To have a feeling of dependence of these distributions on the photon energy ω we present them also for $\omega = 1000\,\text{eV}$. In the latter case the quadrupole effects were studied in [13].

One can see that the distributions rapidly drop with Z. This can be understood by analyzing equation (27). For $Z \geq 2$ the factor $S_1(q,\beta)$ contains the wave function $\Psi(\mathbf{r},\mathbf{r})$ integrated over r in the region of r where the electron density reaches its largest value. This region $r \sim 1/Z$ is the same for the two K shell electrons. Here $\Psi(\mathbf{r},\mathbf{r}) \sim Z^3$. Hence $|S_1(q,\beta)|^2$ is only smoothly dependent on Z. The same does the right hand side of equation (27) for fixed value of ω. For the chosen intervals of ω the Z dependence is contained in the factor $\omega/E^3 \sim 1/Z^4$. The ion H^- is a special case since the densities of the two bound electrons reaches largest values at different values of r. This manifests itself in additional quenching of the wave function $\Psi(\mathbf{r},\mathbf{r})$ and thus of the factor $S_1(q,\beta)$.

The energy distribution of the angular correlation $d\sigma/(d\tau d\beta)$ is given by equation (7). Its value at the point of equal sharing $\beta = 0$ is shown in Figure 3. For the case of helium we include also the result of calculation with the two-exponential approximate functions for the bound state suggested in [16] and employed in [15]. One can see the difference to be small. In Figure 4 we present the angular correlation $d\sigma/d\tau$. The Z dependence of distributions shown in Figures 3 and 4 is smaller than that of the distributions in q^2. They drop as Z^{-2} for $Z \geq 2$ due to the factor p_1p_2 of the first equality on the right hand side of equation (7). The distributions still drop monotonously with Z if we include the case $Z = 1$. As expected, they peak at $\tau = -1$.

In Figure 5 we present the photoelectron energy distributions $d\sigma/d\beta$ at $\beta = 0$ for $\omega \geq 6000\,\text{eV}$ when the QFM is valid for all the objects under discussion: the ion H^- and the heliumlike ions with $2 \leq Z \leq 5$. Following (27) the distributions drop as ω^{-2}. The kinematical factor κ changes from 1.37 at $\omega = 6000\,\text{eV}$ till 1.31 at $\omega = 7000\,\text{eV}$ for $Z = 5$. It varies from 1.09 to 1.07 for H^- in the same energy interval. The main Z dependence is caused by integration of the distribution (27) in $q^2 \sim Z^2$. Thus, Z dependence of distributions $Z^{-2}d\sigma/d\beta$ displayed in Figure 5 is caused by that of the factor $S_1(q,\beta)$. The distribution exhibits slow decrease at $Z \geq 2$. However, for $Z = 1$ it is noticeably smaller than for $Z = 2$. As we discussed earlier, it is due to a smaller probability for the two bound electrons to be at the same space point in the case of H^-.

This can be useful for extension of the analysis carried out in [14] for other values of the photon energies and for other targets.

Now we compare our results with those obtained by other authors for helium at $\omega = 800\,\text{eV}$. The authors of [14] present the differential distribution $d\sigma/d\beta d\tau$. In Figure 2 of [14] they show the energy distribution for $0 \leq \beta \leq 1/2$ integrated over the interval $\pi/6$ around the angle π between the photoelectron momenta. As noted in [14] they can not obtain the absolute values of distribution and normalize the theoretical and experimental results at $\beta = 0$. The theoretical results are obtained by performing numerical computations using the external complex scaling method in the prolate spheroidal coordinates (PSECS) [19]. The scale of Figure 2 of [14] does not

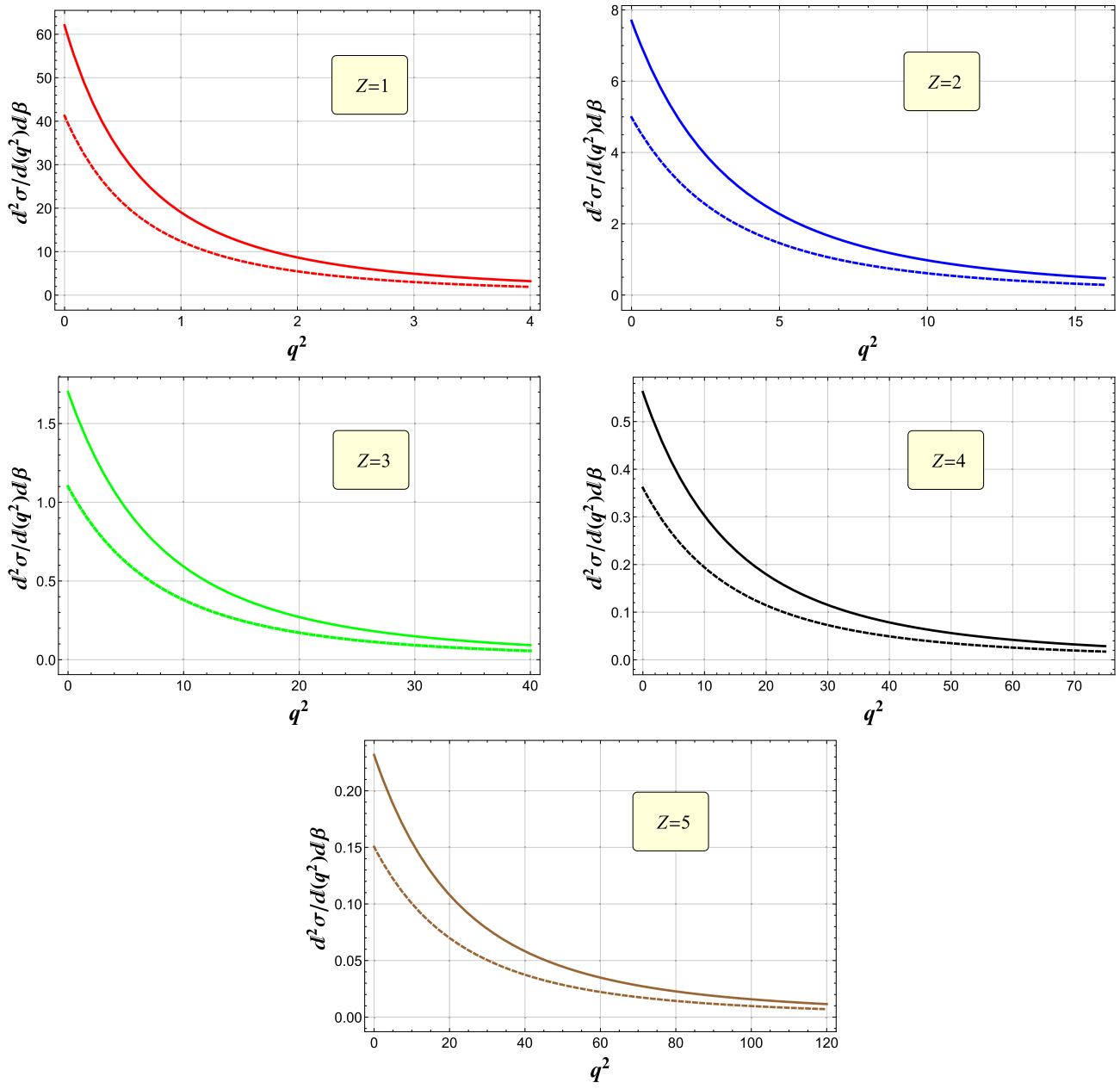

Fig. 1. Distribution $d^2\sigma/d(q^2)d\beta$ in $10^{-10}a_0^4$ is presented as a function of q^2 in a_0^{-2}, where a_0 is the Bohr radius, and $\beta = 0$. The solid lines correspond to the photon energies $\omega = 145, 800, 2000, 3750, 6100\,\text{eV}$, whereas the dashed lines correspond to the photon energies $\omega = 180, 1000, 2500, 4700, 7600\,\text{eV}$ for H^-, He and helium-like ions with $Z = 3; 4; 5$, respectively.

make a detailed analysis possible. Anyway we can estimate the result of [7] as $f(\beta = 0)/f(\beta = 1/2) \approx 2$ for the distribution

$$f(\beta) = \frac{1}{2}\int_{-1}^{-\sqrt{3}/2}\left(\frac{d^2\sigma}{d\tau d\beta}\right)d\tau.$$

In our approach all dependence on β inside the QFM peak is contained in the wave function of the photoelectrons (see Appendix) and thus in the factor $S_1(q^2, \beta)$. Our result is $f(\beta = 0)/f(\beta = 1/2) \approx 1.5$. Thus the energy distribution drops somewhat slower than that found in [14].

The integral $\sigma_{QFM} = \int_0^{1/2} d\beta f(\beta)$ can be identified as the QFM cross section determined by the conditions of experiment [14]. We find $\sigma_{QFM} = 0.222$ barn. Since we neglected the terms of the order β^2 our result is rather $\sigma_{QFM} = 0.22 \pm 0.05$ barns. This is close to the result $\sigma_{QFM} = 0.20$ barn extracted from the paper [9] as presented in Table 1 of [14] being at least 3 times larger than that obtained in [14]. The result of [9] was obtained by employing the Time Dependent Close Coupling method [20]. Note that it was found earlier (see Ch. 9 of [6] for references) that σ_{QFM} depends strongly on the shape of the wave function of the bound state at somewhat larger

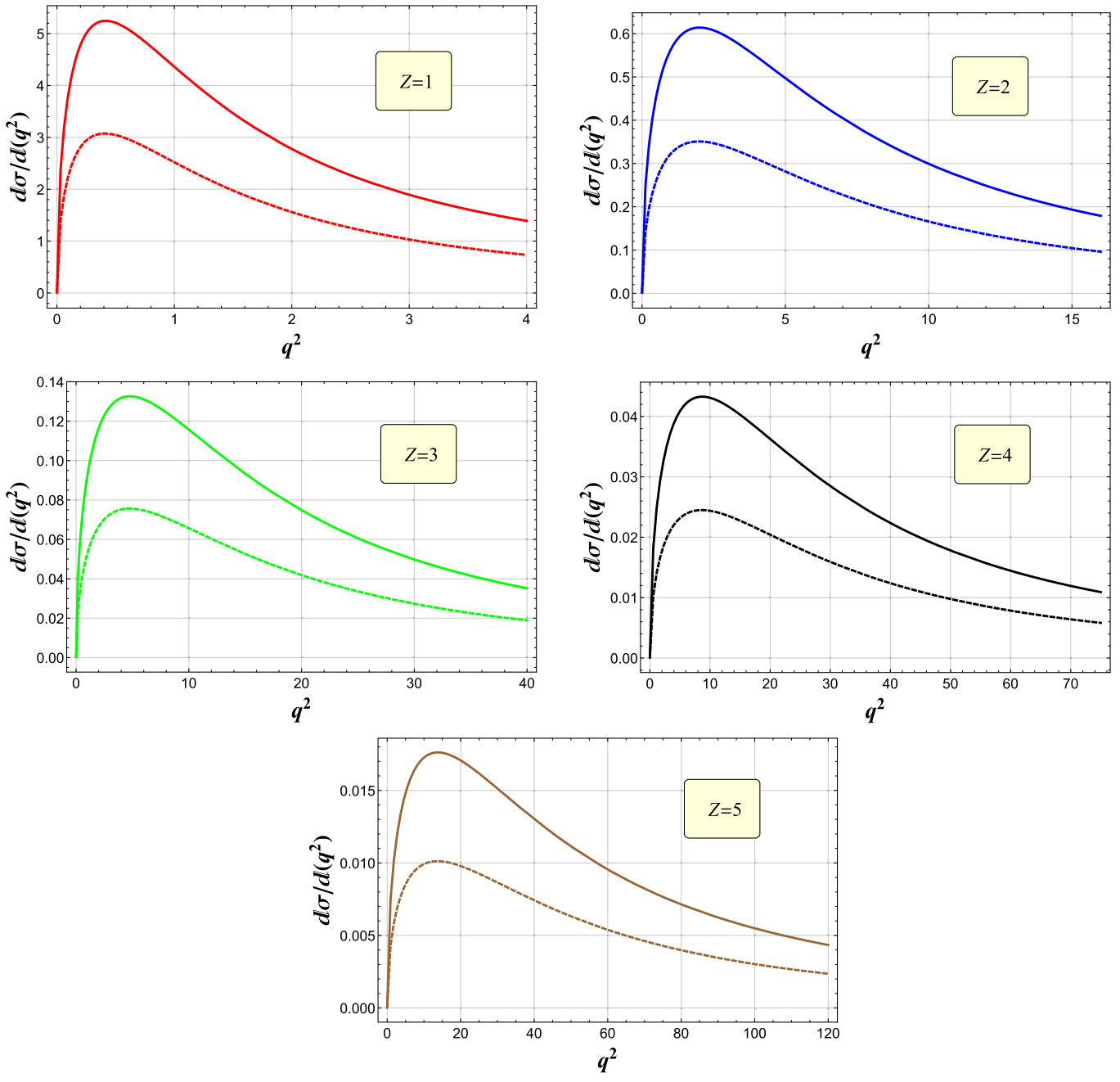

Fig. 2. Distribution $d\sigma/d(q^2)$ in $10^{-10}a_0^4$ is presented as a function of q^2 in a_0^{-2}, where a_0 is the Bohr radius. The solid lines correspond to the photon energies $\omega = 145, 800, 2000, 3750, 6100\,\text{eV}$, whereas the dashed lines correspond to the photon energies $\omega = 180, 1000, 2500, 4700, 7600\,\text{eV}$ for the helium-like atoms with $Z = 1; 2; 3; 4; 5$, respectively.

energies $\omega \geq 6\,\text{keV}$. It is reasonable to expect such dependence to take place for smaller values of ω. It was noted also [10] that σ_{QFM} depends strongly on the shape of the final state wave function.

4 Summary

As it was mentioned above, the QFM predicted 45 years ago [1] was beyond the possibilities of experimental investigations for a long time. The work [7] provided experimental evidence of the existence of QFM. Recent publication [14] presents concrete data on the double and single differential distributions for He atom and for H_2 molecule. This enables us to hope that studies of QFM for other targets will take place transforming a couple of experiments into a whole domain of research that will present data on short range inter-electron correlations in a whole variety of systems of which He, H^- and other helium-like ions form only a small region.

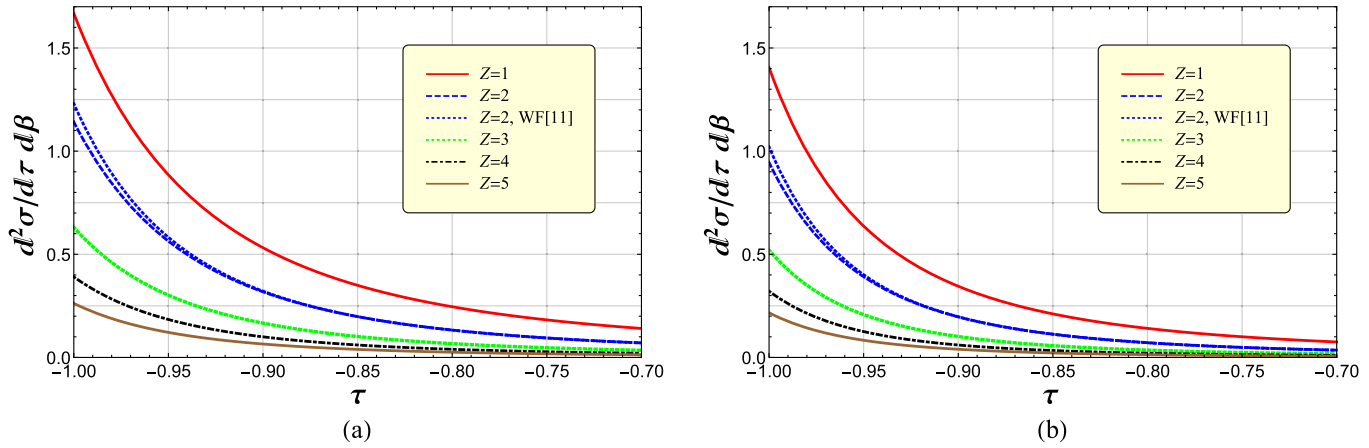

Fig. 3. Distribution $d^2\sigma/d\tau d\beta$ in barns is presented as a function of $\tau = (\mathbf{p}_1 \cdot \mathbf{p}_2)/(p_1 p_2)$ for $\beta = 0$. The curves on the plot (a) correspond to the photon energies $\omega = 145, 800, 2000, 3750, 6100\,\text{eV}$, whereas the curves on the plot (b) correspond to the photon energies $\omega = 180, 1000, 2500, 4700, 7600\,\text{eV}$ for H^-, He and two-electron ions with $Z = 3; 4; 5$, respectively. All curves correspond to the Pekeris-like wave functions [18]. Exception is the case of $Z = 2$ which is additionally presented by the dotted curve (blue online) calculated on the base of the two-exponential ansatz [16].

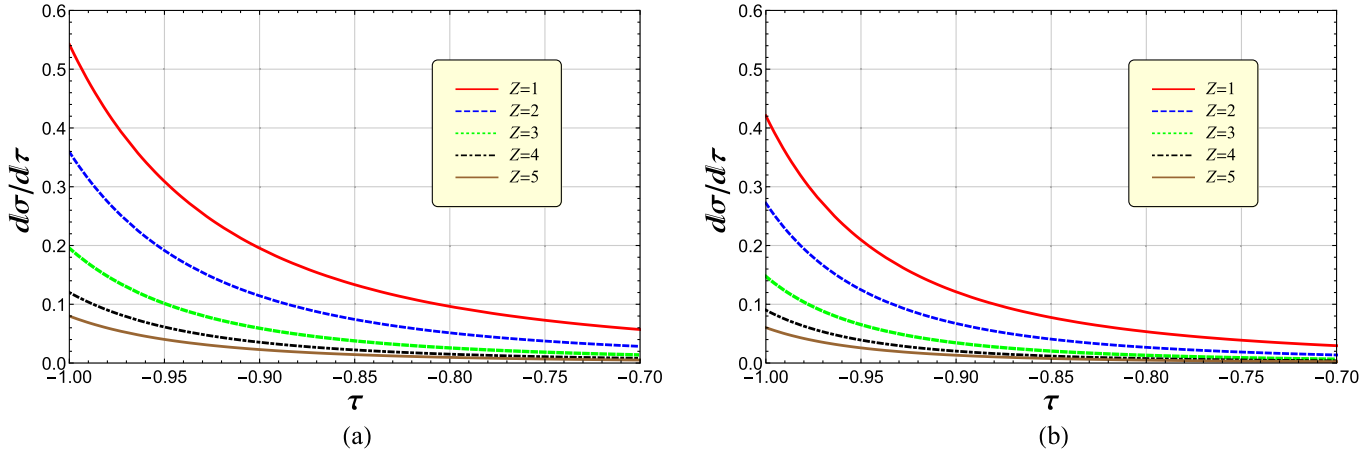

Fig. 4. Distribution $d\sigma/d\tau$ in barns is presented as a function of τ. The curves on the plot (a) correspond to the photon energies $\omega = 145, 800, 2000, 3750, 6100\,\text{eV}$, whereas the curves on the plot (b) correspond to the photon energies $\omega = 180, 1000, 2500, 4700, 7600\,\text{eV}$ for H^-, He and two-electron ions with $Z = 3; 4; 5$, respectively.

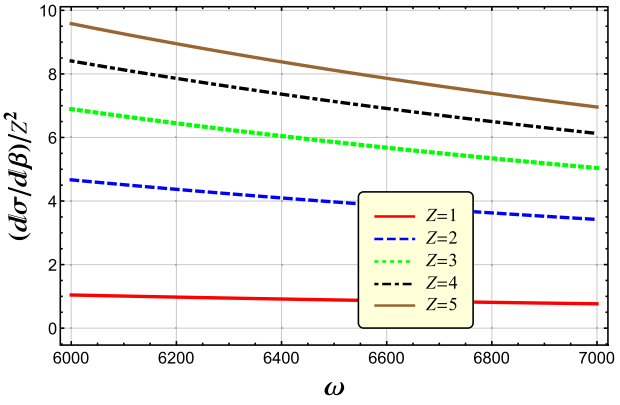

Fig. 5. Distribution $(d\sigma/d\beta)/Z^2$ (see Eq. (4)) in 10^{-4} barns is shown as a function of the photon energy ω (in eV) for the helium-like isoelectronic sequence with $1 \le Z \le 5$ (a_0 is the Bohr radius).

The QFM is interesting from several points of view. It probes the wave function between the bound electrons at small distances and provides a good test for the wave functions at the electron-`electron` coalescence line. The QFM depends on the proper inclusion of correlations of the bound state electrons. It can not be reproduced by uncorrelated bound state functions [6]. The QFM is the only mechanism of ionization which requires going beyond the dipole approximation since it takes place only if the quadrupole terms in photon-electron interaction are included.

This stimulated us to calculate various characteristics of the double photoionization for the negative ion H^-, He atom and for two-electron ions Li^+, Be^{++} and B^{+3} with $Z = 3, 4, 5$, respectively in the region of QFM domination at the photon energies $I \ll \omega \ll \mu$. We trace the Z dependence for the double differential distribution. For He we traced the dependence of the photoelectron energy distribution on the photon energy. Since the interest to

the QFM renewed recently[14], [21] we hope these data to be useful.

Author contribution statement

MA, ED and EL contributed equally on each step of activity that resulted in the appearance of this paper from first idea to the final touches to the manuscript.

Appendix A

In this Appendix we present the refined formula for calculation of the three-dimensional integral $S_1(q,\beta)$ defined by equation (27).

Inserting representations (25) into the RHS of equation (27), we obtain

$$S_1(q,\beta) = N(\xi_1)N(\xi_2)\int d^3R\, e^{i\mathbf{qR}}\, {}_1F_1(i\xi_1,1,ip_1R-i\mathbf{p}_1\mathbf{R})\, {}_1F_1(i\xi_2,1,ip_2R-i\mathbf{p}_2\mathbf{R})\tilde{\Psi}(R,0), \quad (A.1)$$

where $\tilde{\Psi}(R,0)$ represents the two-electron wave function (in the ground state) at the electron-electron coalescence line. The integral (A.1) can be easily calculated for $\tilde{\Psi}(R,0)$ presented in the form

$$\tilde{\Psi}(R,0) = \sum_{j=1}^{n} C_j \exp(-\lambda_j R). \quad (A.2)$$

The Pekeris-like wave functions which we applied [17,18] do not have the form (A.2) at the electron-electron coalescence line. However, fortunately, it is sufficient to include five separate exponential terms ($n = 5$) to obtain extremely accurate wave function $\tilde{\Psi}(R,0)$ of the form (A.2) by fitting the Pekeris-like wave functions with the number of shells $\Omega = 25$ [18].

It follows from equations (A.1) and (A.2) that calculations of the integral (A.1) reduce to computation of the integral

$$I(q,\beta;\lambda,s) = \int e^{i\mathbf{qR}-\lambda R}\, {}_1F_1(i\xi_1,1,ip_1R-i\mathbf{p}_1\mathbf{R})\, {}_1F_1(i\xi_2,1,ip_2R-i\mathbf{p}_2\mathbf{R})R^s d^3R. \quad (A.3)$$

It is clear that the analytic form for the latter integral with $s = 0$ can be obtain by differentiation of the integral (A.3) with $s = -1$, in respect to parameter λ. The analytic form of the integral $I(q,\lambda,-1)$ was derived in reference [22]. Now we employ this result and take into account that integral (A.1) depends, in fact, only on q^2. The evaluation mentioned above provides the required integral in the form

$$\begin{aligned} I(q,\beta;\lambda,0) = {} & -4\pi\left(\lambda^2+q^2\right)^{i(\xi_1+\xi_2)-1}(p_2-p_1-i\lambda)^{-i\xi_1} \\ & (p_1-p_2-i\lambda)^{-i\xi_2}(p_1+p_2+i\lambda)^{-i(\xi_1+\xi_2)} \\ & \times\Bigg\{ {}_1F_1\left[i\xi_1+1,i\xi_2+1;2;h(q,\beta,\lambda)\right] \\ & \frac{2\lambda\xi_1\xi_2 h(q,\beta,\lambda)}{(p_1-p_2)^2+\lambda^2} + {}_1F_1\left[i\xi_1,i\xi_2;1;h(q,\beta,\lambda)\right]\times \\ & \left(\frac{\xi_1+\xi_2}{p_1+p_2+i\lambda}+\frac{\xi_1}{p_1-p_2+i\lambda}+\frac{\xi_2}{p_2-p_1+i\lambda}\right. \\ & \left.+\frac{2\lambda[i(\xi_1+\xi_2)-1]}{\lambda^2+q^2}\right)\Bigg\}, \end{aligned} \quad (A.4)$$

where

$$h(q,\beta,\lambda) = 1-\frac{\lambda^2+q^2}{(p_1-p_2)^2+\lambda^2}, \quad (A.5)$$

and $p_1 = \sqrt{mE(1+\beta)}$, $p_2 = \sqrt{mE(1-\beta)}$.

References

1. M.Ya. Amusia, E.G. Drukarev, V.G. Gorshkov, M.P. Kazachkov, J. Phys. B **8**, 1248 (1975)
2. E.G. Drukarev, F.F. Karpeshin, J. Phys. B **9**, 399 (1976)
3. R. Krivec, M.Ya. Amusia, V.B. Mandelzweig, Phys. Rev. A **64**, 052708 (2001)
4. T. Surić, E.G. Drukarev, R.H. Pratt, Phys. Rev. A **67**, 022709 (2003)
5. T. Kato, Commun. Pure Appl. Math. **10**, 151 (1957)
6. E.G. Drukarev, A.I. Mikhailov, *High Energy Atomic Physics* (Springer International Publishing, Switzerland, 2016)
7. M.S. Schöffler et al., Phys. Rev. Lett. **111**, 0132003 (2013)
8. A.Y. Istomin, A.F. Starace, N.L. Manakov, A.V. Meremianin, A.S. Kheifets, I. Bray, J. Phys. B **39**, L35 (2006)
9. J.A. Ludlow, J. Colgan, T.G. Lee, M.S. Pindzola, F. Robicheaux, J. Phys. B **42**, 225204 (2009)
10. A.G. Galstyan, O. Chuluunbaatar, Yu.V. Popov, B. Piraux, Phys. Rev. A **85**, 023418 (2012)
11. T. Jahnke et al., J. Electron Spectrosc. Relat. Phenom. **141**, 229 (2004)
12. V. Viefhaus et al., Nucl. Instrum. Methods Phys. Res. A **477**, 256 (2002)
13. S. Grundmann et al., Phys. Rev. Lett. **121**, 173003 (2018)
14. S. Grundmann et al., Phys. Rev. Lett. [submitted], arXiv:2001.07713 (2020)
15. M.Ya. Amusia, E.G. Drukarev, E.Z. Liverts, A.I. Mikhailov, Phys. Rev. A **87**, 043423 (2013)
16. E.Z. Liverts, M.Ya. Amusia, R. Krivec, V.B. Mandelzweig, Phys. Rev. A **73**, 012514 (2006)
17. E.Z. Liverts, N. Barnea, Comput. Phys. Commun. **182**, 1790 (2012)
18. E.Z. Liverts, N. Barnea, Comput. Phys. Commun. **184**, 2596 (2013)
19. V.V. Serov, B.B. Joulakian, Phys. Rev. A **80**, 062713 (2009)
20. M.S. Pindzola et al., J. Phys. B **40**, R39 (2007)
21. S.G. Chen et al., Phys. Rev. Lett. **124**, 043201 (2020)
22. A. Nordsieck, Phys. Rev. **93**, 785 (1954)